A compact combined ultrahigh vacuum scanning tunnelling microscope (UHV STM) and near-field optical microscope

2008 Meas. Sci. Technol. 19 045301

(http://iopscience.iop.org/0957-0233/19/4/045301)

Meas. Sci. Technol. **19** (2008) 045301 (7pp) doi:10.1088/0957-0233/19/4/045301

A compact combined ultrahigh vacuum scanning tunnelling microscope (UHV STM) and near-field optical microscope

R A J Woolley[1,2], J A Hayton[1], S Cavill[1,3], Jin Ma[1], P H Beton[1] and P Moriarty[1]

[1] School of Physics and Astronomy, University of Nottingham, Nottingham NG7 2RD, UK
[2] Nanograph Systems Ltd, BioCity Nottingham, Pennyfoot Street, Nottingham NG1 1GF, UK

E-mail: richard.woolley@nanographsystems.co.uk and philip.moriarty@nottingham.ac.uk

Received 29 September 2007, in final form 12 November 2007
Published 7 February 2008
Online at stacks.iop.org/MST/19/045301

Abstract
We have designed and constructed a hybrid scanning near-field optical microscope (SNOM)–scanning tunnelling microscope (STM) instrument which operates under ultrahigh vacuum (UHV) conditions. Indium tin oxide (ITO)-coated fibre-optic tips capable of high quality STM imaging and tunnelling spectroscopy are fabricated using a simple and reliable method which foregoes the electroless plating strategy previously employed by other groups. The fabrication process is reproducible, producing robust tips which may be exchanged under UHV conditions. We show that controlled contact with metal surfaces considerably enhances the STM imaging capabilities of fibre-optic tips. Light collection (from the cleaved back face of the ITO-coated fibre-optic tip) and optical alignment are facilitated by a simple two-lens arrangement where the in-vacuum collimation/collection lens may be adjusted using a slip-stick motor. A second in-air lens focuses the light (which emerges from the UHV system as a parallel beam) onto a cooled CCD spectrograph or photomultiplier tube. The application of the instrument to combined optical and electronic spectroscopy of Au and GaAs surfaces is discussed.

Keywords: scanning tunnelling microscopy, near-field scanning microscopy and spectroscopy, metallic surfaces, semiconductor surfaces

(Some figures in this article are in colour only in the electronic version)

1. Introduction

Scanning probe microscopy (SPM) has evolved to the point where it is now almost routine for a number of physicochemical properties to be imaged simultaneously. In addition to the well-known variants of the tapping/non-contact topographic SPM mode which involve monitoring force-gradient derived shifts in the resonant frequency of the cantilever, an exciting hybrid of optical and scanning probe imaging was realized some time ago in the form of the scanning near-field optical microscope (SNOM). Although the original SNOM design [1] used a scanning tunnelling microscope (STM) to regulate the tip–sample separation, the vast majority of modern SNOM instruments employ shear force methods. Tunnel current-based feedback has largely been avoided not only due to the drive to apply the SNOM to a range of systems which are difficult or impossible to study with STM, but also because of the difficulties associated with maintaining stable STM feedback while tunnelling through adsorbed layers on surfaces under atmospheric conditions[4]. This is somewhat unfortunate as an ultrahigh vacuum (UHV) STM represents, from a number of perspectives, perhaps the most powerful scanning probe: not only is it possible with the STM to image atoms and molecules

[3] Current address: Diamond Light Source Ltd, Diamond House, Harwell Science and Innovation Campus, Didcot, Oxfordshire OX11 0DE,UK.

[4] We focus here only on aperture SNOM; apertureless SNOM using STM feedback control has been demonstrated by a number of groups [2–4].

adsorbed on a surface, but also by careful control of tip–surface interactions, individual adsorbates may be controllably positioned.

There is also a substantial, and growing, body of work on STM-excited light emission, a technique pioneered by Gimzewski *et al* [5] and Berndt *et al* [6] in the late eighties and early nineties. A wide range of samples and materials have now been studied using tunnelling-induced photon emission, including metals [6–8], semiconductor surfaces [9–11] and low dimensional structures [12–14], conjugated polymers [15, 16] and adsorbed molecules [17–20]. A number of approaches to the collection of the photons emitted from the tunnel junction have been adopted by different groups. The original configuration in Gimzewski *et al*'s pioneering experiments [5] involved placing a photomultiplier tube as close as possible to the tunnel junction. Since that work, various methods of increasing the light collection efficiency have been proposed. Berndt *et al* [7, 21, 22] implemented a lens-based system which has been widely adopted. Ellipsoidal mirrors [23, 24] and optical fibres [10, 25–27] have also been used. In each case, the photons are collected in the optical far field.

In 1995 Murashita and Tanimoto [28] introduced a novel *near-field* collection geometry where a conducting and optically transparent tip is used both to acquire STM images and to collect light. Fibre-optic tips coated by a gold/indium oxide layer were shown to have a sufficiently low resistivity and high optical transmittance to enable the collection of tunnelling electron-induced luminescence from bulk GaAs [29]. Moreover, the tip design pioneered by Murashita [29] has proven to be capable of providing atomic resolution images of semiconductor surfaces [30]. Fujita *et al* have also adopted the transparent probe approach [31] and have used indium tin oxide (ITO) as the coating material. In addition to the ITO film, they deposit a thin (∼20 nm) layer of Ag to improve STM luminescence efficiency [31]. Alternative techniques for the formation of transparent and conductive probes based on tin oxide have been published by Tätte *et al* [32] and Jacobsen *et al* [33]. Nakajima *et al* [34] proposed a 'double metal film' procedure involving two Pt coatings to improve the radius of curvature (without sacrificing optical throughput) of the fibre-optic tip. Most recently, Murashita has developed a conductive transparent fibre probe for shear-force AFM operation [35] so that the optical and electronic properties of both conductive and insulating sample regions can be measured in parallel.

In this paper, we describe the design and development of a compact UHV SNOM–STM instrument which utilizes ITO-coated fibre-optic tips similar to those introduced by Murashita [29]. Our tip preparation strategy differs from that put forward by Murashita, enabling a higher rate of tip production. Furthermore, in both the Murashita [29] and Fujita *et al* [31] designs, light collection from the transparent tip is achieved via fibre-optic feedthroughs and couplers. We introduce an alternative approach where light is collected from the cleaved end of the fibre tip using a lens system. We also show, for the first time, that ITO-coated fibre-optic tips are capable of both high quality *I–V* spectroscopy and controlled nanoscale surface modification.

2. Instrument development

A key guiding principle in the design of the SNOM–STM was simplicity. We were keen to ensure that the optical elements, in addition to not compromising the scanning probe performance, could be adjusted for maximum throughput quickly and reliably. In this we have been successful: following a removal of the SNOM–STM from the UHV chamber with subsequent reinstallation, it takes a matter of minutes for the optics to be realigned (in the event that realignment is necessary). Moreover, we decided to forego the multiple optical fibre/multi-connector arrangement used by Murashita [29], instead opting for a simple two-lens (collector/collimator, focusing) set-up. This type of two-lens arrangement has been exploited very successfully in photon emission STM instruments, where the focus of the first lens is at the tip–sample junction [22, 23]. In our case, the focus of the collector is at the cleaved (back) face of the fibre tip. Before describing the SNOM–STM instrument in detail, we first discuss our SNOM–STM tip preparation technique as it differs in a number of key aspects from previously published protocols [29].

2.1. SNOM–STM tip preparation

In addition to requiring that the tip be optically transparent with an aperture whose dimensions are between a few tens and a few hundred nanometres (as is the case for conventional SNOM work), SNOM–STM tips must of course also be electrically conducting. As discussed above, Murashita [29] and Fujita *et al* [31] have used tin oxide or ITO as the transparent conductive coating. This method has given rise to robust probes capable of stable tunnelling and high quality imaging and optical spectroscopy (under both ambient conditions and in UHV). We have modified the tip preparation process described by Murashita [29], yielding a substantial decrease in the time (and complexity) associated with producing SNOM–STM tips. A set of 32 tips can now be produced in a day.

We have used pipette pulling [36] methods with a commercial micropipette puller (Sutter Instruments P-2000) to produce sharp fibre tips. Although the tip shape is heavily dependent on the pulling parameters, these are easily controlled and highly reproducible. All tips are prepared from multimode silica fibre (Newport F-MLD, core diameter: 100 μm, numerical aperture: 0.22, optimized for transmission at 850 nm). As our initial 'commissioning' experiments for the instrument focused on photoluminescence measurements of bulk GaAs, the optimal transmission wavelength of the F-MLD fibre was close to ideal.

Once a set of tips has been produced, they are held securely between two metal plates to be mounted in the sputterer chamber. After sputter coating a film of indium tin oxide (the tip is not rotated during sputtering), the length of the fibre is coated by a further conducting layer which electrically connects the surface of the ITO fibre to a tantalum tip nut via a metal capillary (see figure 1). Other groups [29] have reported the use of electroless plating of copper or nickel, which requires the tip region to be coated in an epoxy resin—a

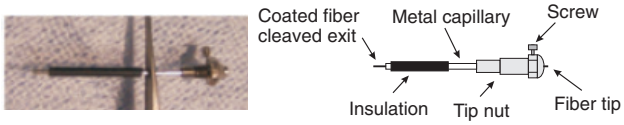

Figure 1. A photograph and a schematic diagram of the ITO-coated fibre-optic tips used in the SNOM–STM instrument. The schematic diagram shows the various components of the tip 'unit'. The vertical bar in the photograph is a pair of tweezers holding the tip in place.

tricky and time-consuming process. Our approach is to coat the fibre by hand (to a distance of order 100 μm from the tip) with a layer of conducting UHV epoxy (Epoxy Technology H20E), first diluted with acetone to allow an even, thin coating. This strategy requires annealing at 150 °C to cure the UHV epoxy—a heating step which also improves the conductivity of the ITO film (as ascertained from four probe electrical measurements). Takayama *et al* [37] have similarly observed a considerable drop in the resistivity of ITO films annealed at 150 °C. Following the epoxy coating step, the fibre tip is carefully inserted into a metal capillary tube which in turn is held in place in the tip nut by a grub screw (see figure 1). The tip nut can then be transported by in-vacuum tools for tip transfer.

SEM images of ITO-coated tips are shown in figure 2. As noted above we find that the fibre pulling process is reproducible, yielding radii of curvature of order 100 nm and cone angles of between 20° and 25°. It is important to note, however, that as the ITO film thickness we currently use is also approximately 100 nm (see figure 2(*b*)), it is likely that the radius of curvature of the uncoated tip is somewhat less than 100 nm.

2.2. The SNOM–STM instrument

Figure 3 shows both a photograph of the rear view of the instrument and a CAD 'overview' of the design. A magnet mounting ring is rigidly attached to the four posts seen in figure 3(*b*) which, when combined with oxygen-free high conductivity (OFHC) copper fins on the microscope stage,

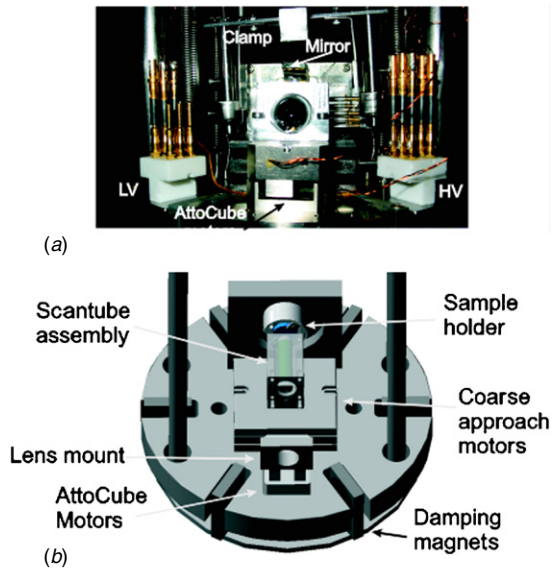

Figure 3. A photograph and CAD drawing of the SNOM–STM instrument. The photograph is a 'rear-view' perspective on the microscope where the lens used for light collection from the fibre tip is at the centre of the image. In (*b*) the springs, mirror and clamping mechanism have been omitted for clarity.

provided eddy current damping. The microscope stage itself, made of 12 mm thick titanium, was suspended from the four posts by springs. Titanium was chosen because it has slightly better thermal properties than stainless steel and reduces differential expansion between microscope components. (The majority of other items on the stage are also manufactured from Ti.)

2.3. Optical set-up

The collection lens for the light emerging from the back face of the fibre tip is mounted at the rear of the microscope on commercial (AttoCube) piezomotors (see figure 3). These motors give a maximum displacement of ±2.5 mm. The fine adjustment capabilities of the lens' motion far exceed

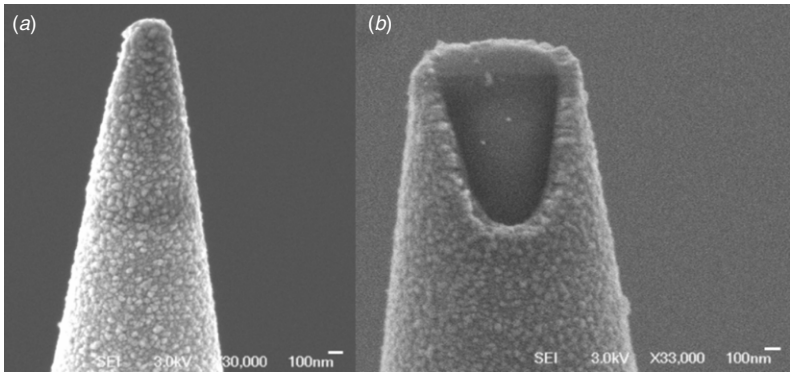

Figure 2. Scanning electron micrographs of ITO-coated fibre-optic tips (scale bar in each case is 100 nm). (*a*) The radius of curvature of the tip is approximately 100 nm with a cone angle of approximately 22°. Note that although the ITO thin film has a grainy morphology, its resistivity is such that STM imaging is possible, albeit difficult, with no further treatment of the tip. (*b*) From the SEM image of a broken tip, the thickness of the ITO film is seen to be of order 100 nm.

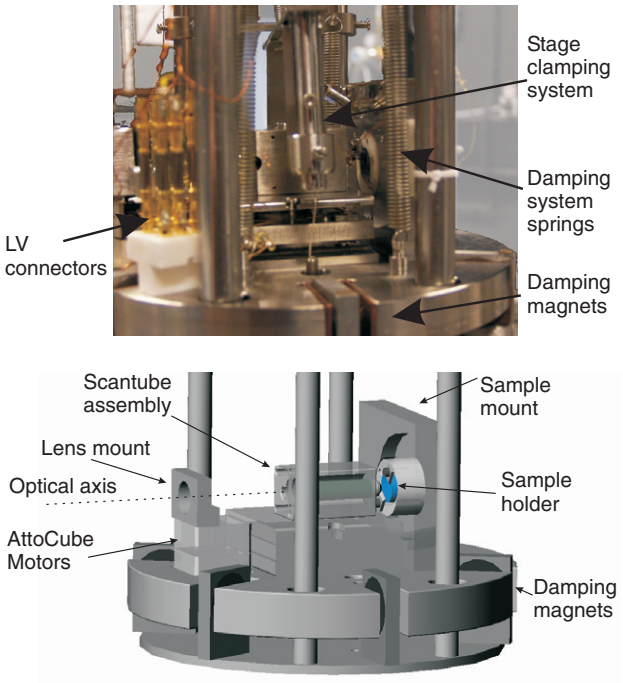

Figure 4. A 'side-on' view of the SNOM–STM instrument. (LV: low voltage). The CAD drawing shows the primary elements of the microscope but, as for figure 3, omits springs, wiring and the clamping mechanism. Moreover, the CAD drawing does not include the small plane mirror mounted above the tip–sample junction which, as described in the text, provides an alternative optical pathway.

requirement but allow for the easy refocusing of the lens on the back face of the fibre tip while maintaining UHV conditions. The dark centre of the lens mount in figure 3 is, in fact, the magnified image of the rear of the scantube assembly.

Maintaining open optical access was obviously key in the development of the system and its successful implementation is demonstrated in the side view of the microscope head, figure 4. In addition to 'side-on' (or grazing incidence) optical access, a small plane mirror is mounted above the tip–sample junction (see figure 3(*a*)). This mirror serves two purposes: (i) the tip–sample distance during the coarse approach can be monitored by a video camera focused on the tip's reflection in the sample and (ii) it provides an alternative optical path for laser excitation.

Light from the rear of the fibre could be collected either in an 'illumination-collection' mode, where both illuminating and collected light passed through the fibre, or in a collection mode, where the laser light, from an inexpensive 5 mW 635 nm diode module, was focused at grazing incidence to a ∼50 μm spot size at the tip–sample junction. The collection lens, when focussed on the cleaved back face of the fibre tip, produces a collimated beam such that at 1.5 m from the UHV viewport the speckle pattern of the multimode fibre is 15 mm in diameter (see figure 5). The beam was then focussed (with a second in-air lens) onto either a photomultiplier or a CCD spectrometer. A Peltier-cooled (−55 °C) CCD spectrograph (Andor Technology) with a 600 lines/mm grating blazed at

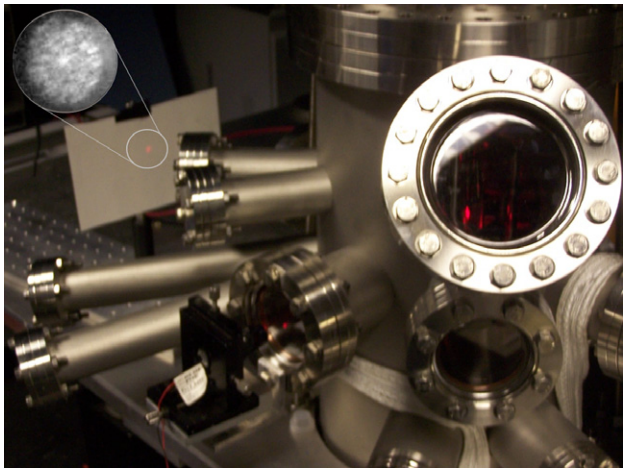

Figure 5. A photograph of laser light captured by the fibre-optic tip and emerging from the cleaved end of the fibre as a parallel beam through the UHV viewport. The spot visible in the upper left corner of the photo (and highlighted in the photograph) is the parallel beam. The inset shows the magnified speckle pattern of the multimode fibre observed in the spot.

700 nm was used for optical spectroscopy, including the photoluminescence measurements of GaAs described in the following section. (The quantum efficiency of the CCD device at 870 nm (i.e. the band gap of bulk GaAs) is approximately 0.35.) A multi-alkali photomultiplier tube (PMT) (LOT Oriel) with a spectral range of 310–850 nm was used to take readings of total emitted light intensities. It is important to note that for the preliminary experiments reported here, the PMT was not cooled. This absence of cooling led to a very significant dark count (∼1000 counts per second). Electronics and software developed in-house [38] were used to control the SNOM–STM instrument, and a simple 'hand-shaking' protocol involving TTL pulses was used to facilitate communication between the microscope controller and the photomultiplier tube/spectrometer software.

3. Instrument commissioning: imaging and spectroscopy of Au(1 1 1) and GaAs(1 0 0) surfaces

To commission the instrument we focussed on acquiring STM images, tunnelling spectra and optical spectroscopy measurements from 'standard' samples, namely Au(1 1 1) films on mica and (passivated) GaAs surfaces.

3.1. Au(1 1 1)

Figure 6(*a*) shows an image of a Au(1 1 1) surface acquired with an 'as-prepared' and unconditioned ITO-coated fibre tip under UHV conditions. With ITO-coated fibre-optic probes, although it was always possible to reach the tunnelling regime and maintain stable feedback with the tip 'parked' at the centre of the image frame, scanning with an unconditioned ITO-coated probe generally—but not exclusively—led to noisy and unstable images such as that shown in figure 6(*a*). Dramatic improvements in imaging and tunnelling stability

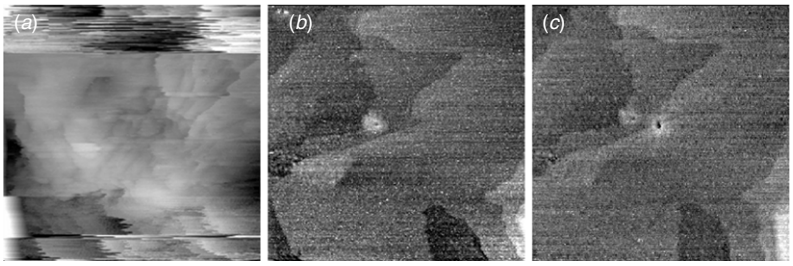

Figure 6. STM images of a Au(1 1 1) sample taken with ITO-coated fibre-optic tips. (*a*) A typical image (300 × 300 nm^2) taken with an 'as-prepared' ITO-coated tip ($V_b = -0.75$ V, $I_t = 0.5$ nA). Scanning results in a significant number of image discontinuities and a substantial level of feedback loop instability. (*b*) A 75 × 75 nm^2 image taken following a 'controlled crash' procedure as described in the text. The raised feature at the centre of the image arises from the tip crash. (*c*) Repetition of the controlled crash procedure produces a hole in this case. The parameters for (*b*) and (*c*) were $V_b = -0.75$ V and $I_t = 0.5$ nA, respectively.

were possible by disengaging the feedback loop and ramping the probe forward ∼10 nm, controllably bringing the tip into contact with the Au(1 1 1) surface. Figure 6(*b*) shows the result of tip–sample contact of this type. A protrusion close to the middle of the image has been produced but, more importantly, the atomic steps of the Au(1 1 1) surface are now clearly visible—the image quality has improved dramatically. A second controlled tip–sample contact in the same sample area resulted in the feature shown in figure 6—in this case, a hole was created. Interestingly, in each case, the feature size is significantly smaller than the nominal 100 nm radius of curvature of the fibre-optic tip.

Following the procedure which produced the hole visible at the centre of figure 6(*c*), a short period of scanning (∼15 min) led to a further significant improvement in the image quality. The inset in the upper left of figure 7 is a 300 × 300 nm^2 image of Au(1 1 1), showing a large number of atomic steps. With the enhancement in imaging capability, high quality and highly reproducible $I(V)$ spectroscopy with the Au-coated fibre tip also became possible, as is shown in figure 7. With a stabilization voltage of 0.5 V in each case, the set-point tunnel current was set at 0.2, 0.3, 0.5 and 0.7 nA for the spectra labelled as (*a*)–(*d*) respectively in figure 7.

The inset in the lower right corner of figure 7 is a graph of total photon intensity versus tip–sample bias for a set-point tunnel current of 10 nA. As mentioned above, the dark counts were significant for the PMT used for this measurement; the data points shown in figure 7 represent the total background-subtracted counts per second measured by the PMT. The maximum above-background count rate in figure 7, at a bias voltage of 2.5 V, is ∼300 counts per second. However, for a tunnel current of 10 nA, we have also intermittently measured count rates of up to 5000 counts per second (above a background of ∼1000 cps). Similarly, the photon signal can vanish due to apparently relatively minor changes in the tip structure (as ascertained from the quality of the STM image). For the PMT and spectrometer used in our experiments to date, we have not detected photon emission for an as-prepared ITO-coated fibre tip. This is consistent with Fujita *et al*'s observation of a lower tunnelling-induced light intensity on Ag(1 1 1) surfaces for ITO-coated fibre tips as compared to those which had been covered with a thin (20 nm) Ag film [31].

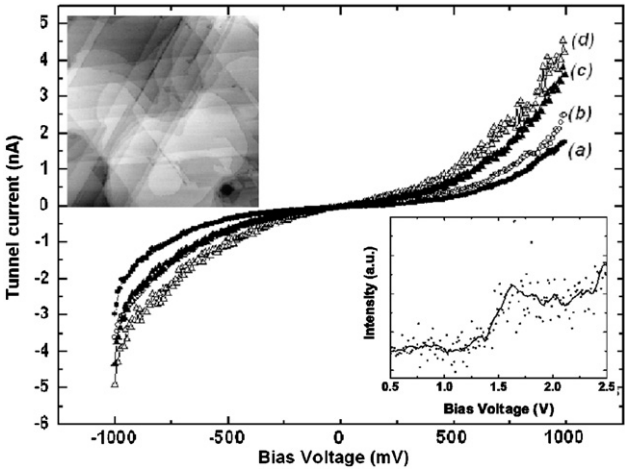

Figure 7. Tunnelling spectra for a Au(1 1 1) surface measured with an ITO-coated fibre tip at various distances from the substrate. (*a*)–(*d*) are taken with set-point (stabilization) currents of 0.2, 0.3, 0.5 and 0.7 nA respectively. The stabilization bias voltage was set at 0.5 V for all spectra. The inset at the top left is an STM image (300 × 300 nm^2) of the Au(1 1 1) surface showing multi- and monatomic steps, whereas that at the bottom right is a spectrum of total light emission (background-subtracted counts per second) from the junction as a function of bias voltage between 0.5 and 2.5 eV. (Tunnel current = 10 nA.) Both the raw data (points) and a second-order Savitzky–Golay smoothed spectrum (solid line) are shown.

As shown by Downes *et al* [39], the threshold voltage for STM-induced photon emission is expected to depend only on the dielectric properties of the materials comprising the tip–sample junction. For Au–Au junctions, the bias threshold is ∼1.4 V [40, 41]. Unfortunately, the lower cut-off energy of the PMT used in our experiments is also 1.45 eV which makes an accurate determination of threshold voltages close to this value problematic. However, it is worth noting that Fujita *et al* [31] observed a shift of the onset voltage for luminescence by ∼1 V (from 2 V to 3 V) when an ITO-coated, as opposed to an Ag/ITO-coated tip, was used to generate STM-induced luminescence from Ag(1 1 1). This, coupled with our observation that light emission only occurs for fibre-optic tips which have been brought into direct contact with the

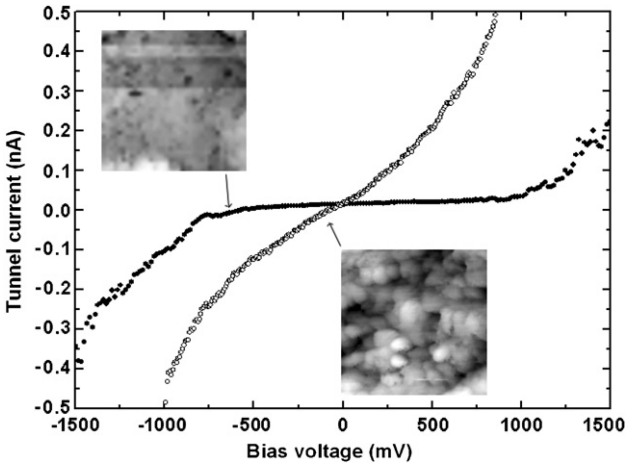

Figure 8. $I(V)$ spectra taken with ITO-coated tips which had previously been brought into contact with Au(1 1 1) surfaces. The filled circles represent the current–voltage characteristic for a $P_2S_5/(NH_4)_2S_x$-treated GaAs(1 0 0) sample, whereas the open circles are the $I(V)$ spectrum for a similarly treated GaAs(1 0 0) surface but with a thin (∼5 nm) Au coating. The inset in the upper left corner is an STM image (200 × 200 nm^2) of the S:GaAs(1 0 0) surface taken with the fibre-optic probe ($V_b = -2$ V, $I_t = 0.5$ nA), whereas the inset in the lower half of the figure is an image (200 × 200 nm^2) of the Au-coated sample.

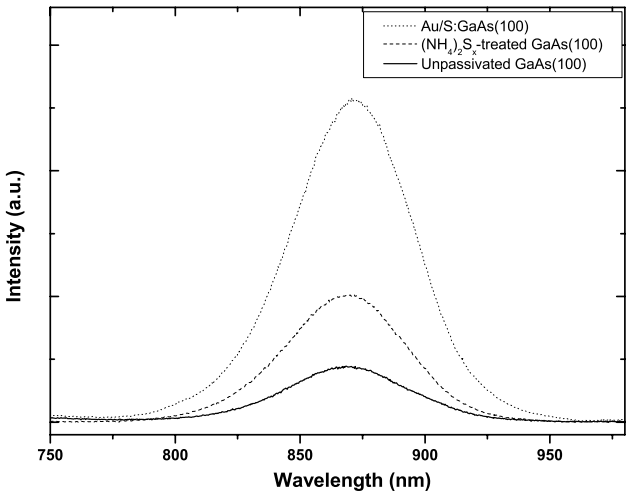

Figure 9. Photoluminescence spectra from GaAs(1 0 0) samples measured with the fibre-optic tip in the tunnelling regime ($V_t = 2.5$ V, $I_t = 0.5$ nA). The tip–sample junction was illuminated by 635 nm light from a laser diode module and the light collected as described in the text. The least intense spectrum (solid line) was acquired from a surface which had been etched in a H_2SO_4:H_2O_2:H_2O solution with no subsequent passivation. Dashed line: PL signal from a $P_2S_5/(NH_4)_2S_x$-passivated sample [42]. Dotted line: PL signal from a $P_2S_5/(NH_4)_2S_x$-passivated sample with a thin (∼5 nm) Au coating.

Au(1 1 1) surface, strongly suggests that the optical spectrum shown in figure 7 arises from a Au–Au tunnel junction.

3.2. Passivated GaAs(1 0 0) surfaces

In figure 8 we plot $I(V)$ characteristics, taken with an ITO-coated fibreoptic probe conditioned as described in the previous section, for two GaAs(1 0 0) surfaces: (i) a $P_2S_5/(NH_4)S_x$-treated (i.e. sulphur-passivated) GaAs(1 0 0) surface, prepared as described by Dagata *et al* [42], and (ii) a sulphur-passivated GaAs(1 0 0) sample with a thin (5 nm) Au film. The purpose of the Au film was to improve the stability against oxidation, and therefore the photoluminescence properties, of the GaAs(1 0 0) surface (see figure 9). Figure 8 also shows STM images of the sulphur-passivated and Au-terminated samples. The $I(V)$ characteristics clearly distinguish between the semiconducting character of the S:GaAs(1 0 0) surface and the metallic properties of the Au-terminated sample.

With the tip in the tunnelling regime, we measured (in the collection mode) the photoluminescence (PL) from passivated and unpassivated GaAs(1 0 0) samples. In each case the PL signal was excited with 635 nm light from a 5 mW laser diode module, focused to an approximate 50 μm spot size, under grazing incidence illumination. As is shown in figure 9, we observe strong differences in PL intensity from sample to sample, as expected for the different surface terminations. The combination of electronic and optical spectroscopy represented by the results of figures 8 and 9 demonstrates the potential of the hybrid instrument we have developed for the analysis of nanostructured and low-dimensional semiconductor systems.

4. Conclusions

We have described a new design for a UHV SNOM–STM, which uses a simple lens arrangement to collect light from ITO-coated fibre-optic probes. The tip fabrication procedure we have discussed is substantially less involved than previously published protocols and enables rapid production of probes. Controlled contact of ITO-coated fibre-optic probes with Au(1 1 1) surfaces leads to significant improvements in their tunnelling spectroscopy and imaging capabilities. Future work will focus on the parallel acquisition of STM images, tunnel current spectra and light emission from adsorbed molecules.

Acknowledgments

We acknowledge funding from the following sources: the Engineering and Physical Sciences Research Council (EPSRC) under grant GR-R34608-1, the EU Framework Programme 6 Marie Curie scheme (under grant MEST-CT-2004-506854 (NANOCAGE)) and the University of Nottingham Interdisciplinary Doctoral Training Centre in Nanoscience.

References

[1] Durig U, Pohl D W and Rohner F 1986 Near-field optical-scanning microscopy *J. Appl. Phys.* **59** 3318–27
[2] Andre P, Charra F and Pileni M P 2002 Resonant electromagnetic field cavity between scanning tunneling microscope tips and substrate *J. Appl. Phys.* **91** 3028–36

[3] Pettinger B, Ren B, Picardi G, Schuster R and Ertl G 2004 Nanoscale probing of adsorbed species by tip-enhanced Raman spectroscopy *Phys. Rev. Lett.* **92** 096101

[4] Barbara A, Lopez-Rios T and Quemerais P 2005 Near-field optical microscopy with a scanning tunneling microscope *Rev. Sci. Instrum.* **76** 023704

[5] Gimzewski J K, Reihl B, Coombs J H and Schlittler R R 1988 Photon-emission with the scanning tunneling microscope *Z. Phys.* B **72** 497–501

[6] Berndt R, Gimzewski J K and Johansson P 1991 Inelastic tunneling excitation of tip-induced plasmon modes on noble-metal surfaces *Phys. Rev. Lett.* **67** 3796–9

[7] Berndt R, Gaisch R, Schneider W D, Gimzewski J K, Reihl B, Schlittler R R and Tschudy M 1995 Atomic-resolution in photon-emission induced by a scanning tunneling microscope *Phys. Rev. Lett.* **74** 102–5

[8] Hoffmann G, Maroutian T and Berndt R 2004 Color view of atomic highs and lows in tunneling induced light emission *Phys. Rev. Lett.* **93** 076102

[9] Downes A and Welland M E 1998 *Phys. Rev. Lett.* **81** 1857–60

[10] Thirstrup C, Sakurai M, Stokbro K and Aono M 1999 Visible light emission from atomic scale patterns fabricated by the scanning tunneling microscope *Phys. Rev. Lett.* **82** 1241–4

[11] Sakurai M, Thirstrup C and Aono M 2004 Optical selection rules in light emission from the scanning tunneling microscope *Phys. Rev. Lett.* **93** 046102

[12] Alvarado S F, Renaud P, Abraham D L, Schonenberger C, Arent D J and Meier H P 1991 Luminescence in scanning tunneling microscopy on iii-v nanostructures *J. Vac. Sci. Technol.* B **9** 409–13

[13] Tsuruoka T, Ohizumi Y, Ushioda S, Ohno Y and Ohno H 1998 *Appl. Phys. Lett.* **73** 1544–6

[14] Evoy S, Harnett C K, Craighead H G, Keller S, Mishra U K and Denbaars S P 1999 *Appl. Phys. Lett.* **74** 1457–9

[15] Lidzey D G, Alvarado S F, Seidler P F, Bleyer A and Bradley D D C 1997 Electroluminescence from a soluble poly(p-phenylenevinylene) derivative generated using a scanning tunneling microscope *Appl. Phys. Lett.* **71** 2008–10

[16] Alvarado S F, Riess W, Seidler P F and Strohriegl P 1997 Stm-induced luminescence study of poly(p-phenylenevinylene) by conversion under ultraclean conditions *Phys. Rev.* B **56** 1269–78

[17] Berndt R, Gaisch R, Gimzewski J K, Reihl B, Schlittler R R, Schneider W D and Tschudy M 1993 Photon-emission at molecular resolution induced by a scanning tunneling microscope *Science* **262** 1425–7

[18] Fujita D, Ohgi T, Deng W L, Ishige K, Okamoto T, Yokoyama S, Kamikado T and Mashiko S 2001 *Surf. Sci.* **493** 702–7

[19] Liu H W, Ie Y, Nishitani R, Aso Y and Iwasaki H 2007 Bias dependence of tunneling-electron-induced molecular fluorescence from porphyrin films on noble-metal substrates *Phys. Rev.* B **75** 115429

[20] Perronet K, Schull G, Raimond P and Charra F 2006 Single-molecule fluctuations in a tunnel junction: a study by scanning-tunnelling-microscopy-induced luminescence *Europhys. Lett.* **74** 313–9

[21] Berndt R, Gimzewski J K and Johansson P 1993 Electromagnetic-interactions of metallic objects in nanometer proximity *Phys. Rev. Lett.* **71** 3493–6

[22] Hoffmann G, Kroger J and Berndt R 2002 Color imaging with a low temperature scanning tunneling microscope *Rev. Sci. Instrum.* **73** 305–9

[23] Berndt R, Schlittler R R and Gimzewski J K 1991 Photon-emission scanning tunneling microscope *J. Vac. Sci. Technol.* B **9** 573–7

[24] Suzuki Y, Minoda H and Yamamoto N 1999 *Surf. Sci.* **438** 297–304

[25] Gallagher M J, Howells S, Yi L, Chen T and Sarid D 1992 Photon-emission from gold surfaces in air using scanning tunneling microscopy *Surf. Sci.* **278** 270–80

[26] Maurel C, Ajustron F, Pechou R, Seine G and Coratger R 2006 *Surf. Sci.* **600** 442–7

[27] Arafune R, Sakamoto K, Meguro K, Satoh M, Arai A and Ushioda S 2001 Multiple-fiber collection system for scanning tunneling microscope light emission spectroscopy *Japan. J. Appl. Phys.* **40** 5450–3

[28] Murashita T and Tanimoto M 1995 Observation of tunneling electron luminescence at low-temperatures using novel conductive transparent tip *Japan. J. Appl. Phys.* **34** 4398–400

[29] Murashita T 1997 Novel conductive transparent tip for low-temperature tunneling-electron luminescence microscopy using tip collection *J. Vac. Sci. Technol.* B **15** 32–7

[30] Yokoyama T and Takiguchi Y 2001 *Surf. Sci.* **482** 1163–8

[31] Fujita D, Onishi K and Niori N 2004 Light emission induced by tunneling electrons from surface nanostructures observed by novel conductive and transparent probes *Microsc. Res. Tech.* **64** 403–14

[32] Tatte T, Avarmaa T, Lohmus R, Maeorg U, Pistol M E, Raid R, Sildos I and Lohmus A 2002 *Mater. Sci. Eng.* C **19** 101–4

[33] Jacobsen V, Tatte T, Branscheid R, Maeorg U, Saal K, Kink I, Lohmus A and Kreiter M 2005 *Ultramicroscopy* **104** 39–45

[34] Nakajima K, Micheletto R, Mitsui K, Isoshima T, Hara M, Wada T, Sasabe H and Knoll W 1999 Development of a hybrid scanning near-field optical/tunneling microscope system *Japan. J. Appl. Phys.* **38** 3949–53

[35] Murashita T 2006 Conductive transparent fiber probes for shear-force atomic force microscopes *Ultramicroscopy* **106** 146–51

[36] Shalom S, Lieberman K, Lewis A and Cohen S R 1992 A micropipette force probe suitable for near-field scanning optical microscopy *Rev. Sci. Instrum.* **63** 4061–5

[37] Takayama S, Sugawara T, Tanaka A and Himuro T 2003 Indium tin oxide films with low resistivity and low internal stress *J. Vac. Sci. Technol.* A **21** 1351–4

[38] Humphry M J, Chettle R, Moriarty P J, Upward M D and Beton P H 2000 Digital scanning probe microscope controller for molecular manipulation applications *Rev. Sci. Instrum.* **71** 1698–701

[39] Downes A, Taylor M E and Welland M E 1998 Two-sphere model of photon emission from the scanning tunneling microscope *Phys. Rev.* B **57** 6706–14

[40] Berndt R and Gimzewski J K 1992 *Surf. Sci.* **269** 556

[41] Olkhovets A, Evoy S and Craighead H G 2000 *Surf. Sci.* **453** L299–302

[42] Dagata J A, Tseng W, Bennett J, Schneir J and Harary H H 1991 *Appl. Phys. Lett.* **59** 3288–90